RAA 2020 Vol. **20** No. **9**, 141(9pp) doi: 10.1088/1674–4527/20/9/141

http://www.raa-journal.org *http://iopscience.iop.org/raa*

***R**esearch in*
***A**stronomy and*
***A**strophysics*

$L_{\rm syn} - E_{\rm syn,p} - \delta$ relation in active galactic nucleus jets and implication for the physical origin of the $L_{\rm p} - E_{\rm p,z} - \Gamma_0$ relation of gamma-ray bursts

Xiao-Li Huang[1,2] and En-Wei Liang[2]

[1] School of Astronomy and Space Science, Nanjing University, Nanjing 210023, China
[2] Guangxi Key Laboratory for Relativistic Astrophysics, School of Physical Science and Technology, Guangxi University, Nanning 530004, China; *lew@gxu.edu.cn*

Received 2020 February 2; accepted 2020 April 7

Abstract High energy photon radiations of gamma-ray bursts (GRBs) and active galactic nuclei (AGNs) are dominated by their jet radiations. We examine whether the synchrotron radiations of jets in BL Lacs, flat spectrum radio quasars (FSRQs), and Narrow Line Seyfert 1 galaxies (NLS1s) follow the relation between the prompt gamma-ray emission and the initial Lorentz factor (Γ_0) of GRBs. It is shown that the AGN sample does not agree with the $L_{\rm p} - E_{\rm p,z} - \Gamma_0$ relation of GRBs. In addition, we obtain a tight relation of $L_{\rm syn} \propto E_{\rm syn,p}^{0.45\pm0.15}\delta^{3.50\pm0.25}$ for FSRQs and NLS1 galaxies, where $L_{\rm syn}$ is the luminosity at peak photon energy $E_{\rm syn,p}$ of the synchrotron radiations. This relation is different from the $L_{\rm p} - E_{\rm p,z} - \Gamma_0$ relation of GRBs. The dependence of $L_{\rm syn}$ to δ is consistent with the expectation of the Doppler boosting effect for the FSRQs and NLS1 galaxies, but it is not for GRBs. We argue that Γ_0 may be a representative of the kinetic power of the radiating region and the tight $L_{\rm p} - E_{\rm p,z} - \Gamma_0$ relation is shaped by the radiation physics and the jet power together.

Key words: gamma-ray burst: general — quasars: general — BL Lacertae objects: general — galaxies: Seyfert — stars: jets — radiation mechanisms: non-thermal

1 INTRODUCTION

Relativistic jets are ubiquitous in the Universe and have been detected in a very diverse range of black hole (BH) systems, ranging from stellar mass to supermassive scale. It is believed that gamma-ray bursts (GRBs) are produced by an ultra-relativistic jet powered by stellar BHs from core collapses of massive stars (e.g., Woosley 1993) or mergers of two compact stars (e.g., Eichler et al. 1989; Paczynski 1991; Kumar & Zhang 2015), and the high energy photon radiations of active galactic nuclei (AGNs) are dominated by radiations from a mildly relativistic jet fed by accretion of their central super-massive BHs (Urry & Padovani 1995; Ghisellini et al. 2009; Zhang et al. 2012, 2015; Liang et al. 2015; Sun et al. 2015; Zhu et al. 2016).

The observed radiations from a jet are boosted by the Doppler effect where the jet is pointed toward the earth. It is generally believed that typical GRBs and blazars, including flat spectrum radio quasars (FSRQs) and BL Lacs, as well as GeV-selected narrow line Seyfert 1 (NLS1) galaxies, are on-axis or small angle off-axis observed to their jets (Urry & Padovani 1995; Kumar & Zhang 2015; Sun et al. 2015; Richards & Lister 2015). Therefore, the Doppler boosting factor (δ) is mainly dependent on the the Lorentz factor (Γ) of a relativistic jet. There are three methods to estimate the initial Lorentz factor (Γ_0) of a GRB fireball. The first is to use the fireball deceleration time derived from the onset peaks observed in early optical afterglow lightcurves (Sari & Piran 1999; Kobayashi et al. 1999; Liang et al. 2010). The second is based on the "compactness" argument by analysing the high energy spectral cutoffs or breaks of the prompt emission of GRBs (Lithwick & Sari 2001; Tang et al. 2015). The third method is to use the photosphere radiation in some GRBs (Pe'er et al. 2007; Peng et al. 2014; Zou et al. 2015). By deriving the Γ_0 values with the first method for a sample of GRBs, Liang et al. (2010) discovered a relation between Γ_0 and the isotropic gamma-ray energy $E_{\rm iso}$ of GRBs. Lü et al. (2012) showed that the isotropic luminosity $L_{\rm iso}$ also depends on Γ_0.

Most of confirmed extra-galactic GeV-TeV sources are blazars. The bimodal feature of their broadband spec-

tral energy distributions (SEDs) is generally represented with the leptonic models of the synchrotron radiation and the inverse Compton (IC) scattering process (e.g., Ghisellini et al. 1996; Urry et al. 1999). The seed photons for the IC process can come from the synchrotron radiation photon field (SSC, Maraschi et al. 1992; Ghisellini et al. 1996; Urry et al. 1999; Zhang et al. 2012) or the external photon field (EC; Sikora et al. 1994, 2009). NLS1 galaxies were identified as a new class of GeV AGNs by the $Fermi$/LAT (Abdo et al. 2009). Their broadband SEDs can also be explained with synchrotron+IC leptonic jet model (Abdo et al. 2009), which are similar to that in FSRQs. In addition, their radiation physics and jet properties are also similar to that in FSRQs (Sun et al. 2015). By modeling the SEDs of 3C 279 (a typical FSRQ) and two NLS1s (PMN J0948+0022 and 1H 0323+342) in different stages, Zhu et al. (2016) found a universal correlation between Doppler factors (δ) and peak luminosities ($L_{\rm c}$) of external Compton scattering bump.

Comparative studies the similarity between the jet radiations from GRBs and AGN outbursts have been presented. A uniform correlation between synchrotron luminosity ($L_{\rm syn}$) and δ in GRBs and blazars is found by Wu et al. (2011). Wang & Wei (2011) showed a similar spectral energy distribution between GRB and AGN jet. Nemmen et al. (2012) illustrated that AGN jets and GRB jets exhibit the same correlation between the jet power and the gamma-ray luminosity, (see also Zhang et al. 2013a; Wang et al. 2014). Such a correlation may be also extended to the jets in black hole X-ray binaries (BXBs) in hard/quiescent states and low-luminosity AGNs with enlarging the range of luminosity more than 20 orders of magnitude, i.e., from 10^{31} to 10^{52} erg s^{-1} (Ma et al. 2014). Furthermore, Zhu et al. (2019) found that the gamma-ray luminosity and power of outflows of short GRBs and pulsar wind nebulae follow that same relation, and the radiation efficiency is independent of the gamma-ray luminosity for various relativistic jet systems. They suggested that the acceleration and emission mechanisms or efficiencies may be similar in all relativistic outflows regardless of their central engines. Lyu et al. (2014) presented a unified picture for the radiation physics of relativistic jets in GRBs and blazars within the framework of the leptonic synchrotron radiation models. Zhang et al. (2017) proposed a potential fundamental plane for low-synchrotron-peak blazar and GRBs.

The distributions of blazars in the $L_{\rm syn,p} - E_{\rm syn}$ plane illustrate as a blazar sequence; i.e., high-luminosity FSRQs tend to have a low peak frequency and low-luminosity BL Lacs tend to have a high peak frequency. This sequence may be related to the different environments of emitting regions for different types of blazars (e.g., Ghisellini et al. 1998). However, a positive correlation between $L_{\rm syn,p}$ and $E_{\rm syn}$ is observed for outbursts in individuals (Massaro et al. 2008; Tramacere et al. 2009; Zhang et al. 2013a). In addition, positive $L_{\rm p} - E_{\rm p,z}$ relations also have been showed in GRBs (Amati et al. 2002; Yonetoku et al. 2004; Liang et al. 2004; Ghirlanda et al. 2004; Lu et al. 2012). Interestingly, Liang et al. (2015) found a tight correlation among the isotropic peak luminosity ($L_{\rm p}$), the peak energy ($E_{\rm p,z}$) of the νf_ν spectrum in the GRBs rest frame, and Γ_0 of GRBs jets. This $L_{\rm p} - E_{\rm p,z} - \Gamma_0$ relation is much tighter than the $L_{\rm p} - E_{\rm p,z}$ relation. This paper investigates whether or not GeV-TeV selected AGNs have a similar $L_{\rm syn} - E_{\rm syn} - \delta$ relation, and explores the possible implications for the physical origin of the $L_{\rm p} - E_{\rm p,z} - \Gamma_0$ relation of GRBs. We present our samples in Section 2. Our analysis results are presented in Section 3. Discussion and conclusions are given in Section 4.

2 SAMPLE AND DATA

Our samples of GeV/TeV-selected FSRQs, BL Lacs, and NLS1s are taken from Zhang et al. (2012, 2015) and Sun et al. (2015). They presented systematical broadband SED fits to these AGNs with the single-zone lepton model. The viewing angle effect significantly influences the measurement of the Doppler factor of a radiating region. Since the jets in these AGNs are only middle relativistic and the viewing angle to the jet axis of blazars is through to be small, it is usually set $\delta = \Gamma$ in modeling the SEDs of blazars (e.g., Zhang et al. 2012, 2014). Using the model parameters reported by Zhang et al. (2012, 2015) and Sun et al. (2015), we obtain the values of Γ, the peak luminosity ($L_{\rm syn}$) and the peak photon energy ($E_{\rm syn,p}$) in the source frame of the synchrotron emission. The bolometric luminosity ($L_{\rm bol}$) of these sources are also calculated with the SED fit results. Note that the model parameters for the BL Lacs are poorly constrained, and no error bars of the parameters are reported in Zhang et al. (2012). Thus, no error is available for our data of BL Lacs. There are 18 FSRQs, 19 BL Lac objects, and five NLS1s are included in our AGN samples. Since these sources are variable, several SEDs in different outbursts are derived for some sources. The data of our AGN samples are reported in Tables 1–3.

Thirty-four GRBs are included in our GRB sample. They are taken from Liang et al. (2015). Liang et al. (2015) calculated the fireball initial Lorentz factors of these GRBs with the observed onset bump in the early optical afterglow lightcurves assuming that the onset bump is due to the deceleration of the fireballs by their ambient medium (Sari et al. 1999). The peak luminosity ($L_{\rm p}$) and the corresponding photon energy ($E_{\rm p}$) of these GRBs are derived

Table 1 Data of Our FSRQs Sample

Name	z	δ	$\log(E_{\rm syn,z})$ (keV)	$\log(L_{\rm syn,52})$ (erg s^{-1})	$\log(L_{\rm bol,52})$ (erg s^{-1})
FSRQs					
3C 279	0.536	12.0±0.5	-4.29 ± 0.15	-5.56 ± 0.05	-4.20 ± 0.01
3C 273	0.158	7.4±0.9	-3.97 ± 0.20	-5.75 ± 0.13	-4.89 ± 0.03
3C 454.3	0.859	17.6 ± 0.6	-4.13 ± 0.10	-4.40 ± 0.10	-2.94 ± 0.01
PKS 1454–354	1.424	20.2 ± 1.8	-3.83 ± 0.40	-4.65 ± 0.4	-3.08 ± 0.04
PKS 0208–512	1.003	15.2 ± 1.3	-4.22 ± 0.40	-5.13 ± 0.40	-3.66 ± 0.02
PKS 0454–234	1.003	20.0 ± 1.9	-4.18 ± 0.30	-5.06 ± 0.30	-3.47 ± 0.02
PKS 0727–11	1.589	20.6 ± 1.2	-3.97 ± 0.20	-4.82 ± 0.15	-3.09 ± 0.03
PKS 0528+134	2.07	18.4 ± 1.3	-4.10 ± 0.20	-4.46 ± 0.14	-3.01 ± 0.06
4C 66.2	0.657	12.2 ± 1.2	-4.21 ± 0.48	-5.59 ± 0.15	-4.23 ± 0.02
4C 29.45	0.729	11.6 ± 1.0	-3.65 ± 0.25	-5.41 ± 0.17	-4.40 ± 0.03
B2 1520+31	1.487	20.8 ± 1.6	-3.99 ± 0.30	-5.27 ± 0.13	-3.36 ± 0.05
PKS 0420–01	0.916	12.8 ± 0.7	-3.66 ± 0.30	-5.23 ± 0.13	-3.99 ± 0.02
1Jy 1308+326	0.997	12.6 ± 0.9	-4.13 ± 0.35	-5.76 ± 0.20	-3.80 ± 0.02
PKS 1510–089	0.36	11.0 ± 0.5	-4.30 ± 0.06	-6.14 ± 0.05	-4.54 ± 0.03
4C 28.07	1.213	14.6 ± 1.1	-4.13 ± 0.20	-5.16 ± 0.17	-3.91 ± 0.02
PMN 2345–1555	0.621	13.8 ± 1.3	-4.30 ± 0.25	-5.87 ± 0.13	-4.54 ± 0.04
S3 2141+17	0.213	8.0 ± 1.0	-3.44 ± 0.30	-5.97 ± 0.11	-5.22 ± 0.02
S4 0133+47	0.859	13.1 ± 1.2	-4.16 ± 0.35	-5.20 ± 0.13	-4.00 ± 0.01
S4 0917+44	2.19	18.2 ± 1.3	-3.92 ± 0.30	-4.54 ± 0.15	-3.23 ± 0.02
PKS 0227–369	2.115	17.8 ± 1.0	-3.79 ± 0.30	-4.69 ± 0.13	-3.20 ± 0.03
PKS 0347–211	2.944	26.2 ± 1.5	-3.74 ± 0.30	-4.25 ± 0.15	-2.87 ± 0.03
PKS 2325+093	1.843	17.6 ± 17.6	-3.33 ± 0.30	-3.90 ± 0.13	-3.16 ± 0.03
PKS 1502+106	1.839	27.0 ± 2.3	-3.98 ± 0.32	-4.40 ± 014	-2.64 ± 0.04

δ is the Doppler boosting factor, $E_{\rm syn,z}$ is the synchrotron peak photon energy in the source frame, $L_{\rm syn}$ and $L_{\rm bol}$ are the synchrotron peak luminosity and bolometric luminosity, respectively. They are derived from the SED fits with the single-zone leptonic model as reported in Zhang et al. (2015).

Table 2 Data of BL Lacs Sample

Name	z	δ	$\log(E_{\rm syn,z})$ (keV)	$\log(L_{\rm syn,52})$ (erg s^{-1})	$\log(L_{\rm bol,52})$ (erg s^{-1})
BL Lacs					
Mkn 421$^{\rm L}$	0.031	29	-0.295	-7.126	-6.201
Mkn 501$^{\rm L}$	0.034	14	-0.914	-7.709	-6.745
Mkn 501$^{\rm H}$	0.034	15	1.871	-6.536	-5.699
W Com$^{\rm L}$	0.102	15	-2.159	-7.090	-6.000
W Com$^{\rm H}$	0.102	14	-2.320	-6.995	-5.553
BL Lacertae$^{\rm L}$	0.069	19	-3.304	-6.937	-6.000
BL Lacertae$^{\rm H}$	0.069	20	-2.979	-7.310	-6.036
PKS 2005–489$^{\rm H}$	0.071	42	-1.633	-6.659	-5.620
1ES 1959+650$^{\rm L}$	0.048	11	0.038	-7.050	-6.180
1ES 1959+650$^{\rm H}$	0.048	12	1.786	-6.741	-6.678
1ES 2344+514$^{\rm L}$	0.044	13	-1.045	-7.898	-7.036
PKS 2155–304$^{\rm L}$	0.116	50	-1.354	-6.137	-5.208
PKS 2155–304$^{\rm H}$	0.116	26	-1.041	-5.876	-4.180
1ES 1101–232$^{\rm L}$	0.186	12	-0.223	-6.459	-5.638
3C 66A	0.44	24	-1.653	-5.396	-3.921
PG 1553+113	0.3	32	-1.696	-5.386	-4.509
1ES 1218+30.4	0.182	20	-0.867	-6.612	-5.638
1ES 1011+496	0.212	13	-0.236	-5.799	-4.959
PKS 1424+240	0.5	33	-1.319	-4.952	-4.180
1ES 0806+524	0.138	12	-1.496	-7.126	-6.161
Mkn 180	0.045	6	-1.092	-8.123	-7.174
RGB J0152+017	0.08	5	-0.236	-8.114	-6.921
H1426+428	0.129	8.5	0.472	-7.264	-5.699
PKS 0548–322	0.069	6	0.263	-7.692	-6.796

δ is the Doppler boosting factor, $E_{\rm syn,z}$ is the synchrotron peak photon energy in the source frame, $L_{\rm syn}$ and $L_{\rm bol}$ are the synchrotron peak luminosity and bolometric luminosity, respectively. They are derived from the SED fits with the single-zone leptonic model as reported in Zhang et al. (2012). Sources marked with "H" or "L" indicate the high and low states as defined in Zhang et al. (2012).

Table 3 Data of NLS1 Sample

Name	z	δ	$\log(E_{\rm syn,z})$ (keV)	$\log(L_{\rm syn,52})$ (erg s^{-1})	$\log(L_{\rm bol,52})$ (erg s^{-1})
NLS1					
1H 0323+342(1)	0.0629	2.8 ± 0.6	-3.96 ± 0.40	-7.32 ± 0.30	-6.30 ± 0.01
1H 0323+342(2)	0.0629	3.6 ± 1.3	-4.43 ± 0.45	-7.52 ± 0.50	-6.52 ± 0.02
1H 0323+342(3)	0.0629	4.9 ± 0.8	-4.62 ± 0.40	-7.29 ± 0.40	-6.37 ± 0.01
1H 0323+342(4)	0.0629	4.5 ± 0.6	-4.80 ± 0.40	-7.34 ± 0.40	-6.26 ± 0.01
1H 0323+342(5)	0.0629	6.2 ± 0.6	-4.76 ± 0.15	-6.98 ± 0.15	-5.95 ± 0.01
PMN J0948+0022(1)	0.5846	11.1 ± 1.4	-4.38 ± 0.42	-5.60 ± 0.25	-4.60 ± 0.02
PMN J0948+0022(2)	0.5846	10.8 ± 1.3	-4.20 ± 0.25	-5.31 ± 0.24	-4.60 ± 0.01
PMN J0948+0022(3)	0.5846	8.6 ± 1.3	-4.22 ± 0.40	-5.68 ± 0.30	-4.79 ± 0.01
PMN J0948+0022(4)	0.5846	11.1 ± 1	-4.48 ± 0.32	-5.38 ± 0.25	-4.65 ± 0.02
PMN J0948+0022(5)	0.5846	11.6 ± 0.8	-4.45 ± 0.25	-5.42 ± 0.15	-4.43 ± 0.02
PMN J0948+0022(6)	0.5846	9.5 ± 0.5	-4.54 ± 0.17	-5.95 ± 0.13	-4.67 ± 0.02
PMN J0948+0022(7)	0.5846	13.5 ± 1.1	-4.89 ± 0.20	-5.32 ± 0.20	-3.76 ± 0.02
PMN J0948+0022(8)	0.5846	13.7 ± 1.8	-5.08 ± 0.45	-5.28 ± 0.34	-3.92 ± 0.02
PMN J0948+0022(9)	0.5846	11.4 ± 2.2	-4.08 ± 0.40	-5.37 ± 0.35	-4.30 ± 0.01
SBS 0846+513	0.5835	7.4 ± 0.8	-4.51 ± 0.15	-6.67 ± 0.09	-5.15 ± 0.03
PKS 1502+036	0.409	9.5 ± 0.8	-4.29 ± 0.20	-6.47 ± 0.15	-5.39 ± 0.08
PKS 2004–447	0.24	6.4 ± 0.5	-4.29 ± 0.15	-6.97 ± 0.10	-6.18 ± 0.02

δ is the Doppler boosting factor, $E_{\rm syn,z}$ is the synchrotron peak photon energy in the source frame, $L_{\rm syn}$ and $L_{\rm bol}$ are the synchrotron peak luminosity and bolometric luminosity, respectively. They are derived from the SED fits with the single-zone leptonic model as reported in Sun et al. (2015). Different flux states of two NLS1 galaxies, 1H 0323+342 and PMN J0948+0022, are also reported in Sun et al. (2015).

from the fits to the observed spectra accumulated in 1-second peak time slice with the Band function or a power law with an exponential cutoff model. The bolometric luminosity in $1 - 10^4$ keV is calculated with the flux from spectral fits to the time-integrated spectra of these GRBs. The data are reported in Table 4.

3 CORRELATION ANALYSIS RESULTS

We conduct a Spearman pair correlation analysis between the luminosity and Doppler boosting factor for each subgroup of the AGNs and for the entire samples of the AGNs and GRBs. Our results are reported in Table 5. It is found that both $L_{\rm syn}$ (or $L_{\rm p}$) and $L_{\rm bol}$ depend on Γ (or Γ_0) with a power-law index ranging from 2.27 to 4.58 for different sub-classes of AGNs. We make correlation analysis for the entire AGN and GRB samples, as shown in Figure 1, the BL Lacs are separated from the FSRQs and NLS1 galaxies, and BL Lacs tend to be dimmer than the FSRQs and NLS1 galaxies with the same Γ. Both GRBs and AGNs shape a clear sequence in the $\log L_{\rm syn} - \log\Gamma$ and $\log L_{\rm bol} - \log\Gamma$ planes. Our correlation analysis yields $L_{\rm syn} \propto \Gamma^{4.64\pm0.20}$, and $L_{\rm bol} \propto \Gamma^{3.20\pm0.17}$ (see also Wu et al. 2011). However, this relation has very large dispersion ($\Delta = 1.20$). Our Spearman correlation analysis between $E_{\rm syn}$ and δ does not reveal any statistical correlation with a chance probability $p < 10^{-4}$ between the two quantities in each subclass of the AGNs.

Physically, the observed luminosity and photon energy are boosted by the jet bulk Doppler effect. As shown in Liang et al. (2015), by incorporating the Doppler boosting factor the derived $L_{\rm p} - E_{\rm p} - \Gamma_0$ relation is much tighter than the $L_{\rm p} - E_{\rm p}$ relation. We first examine whether the synchrotron radiations of the selected AGNs follow the $L_{\rm p} - E_{\rm p,z} - \Gamma_0$ relation of GRBs; i.e., $L_{\rm p} \propto E_{\rm p,z}^{1.34\pm0.14}\Gamma_0^{1.32\pm0.19}$ (Liang et al. 2015). We calculate the synchrotron peak luminosity ($L_{\rm syn}^{\rm r}$) with this relation for the AGNs by using their $E_{\rm syn,p}$ and Γ values. Figure 2 shows $L_{\rm syn}^{\rm r}$ as a function of the observed $L_{\rm syn}$. It is found that the BL Lacs are in the low luminosity end of this relation with a very large scatter, and the derived $L_{\rm syn}^{\rm r}$ of FSRQs and NLS1 galaxies are 4–5 orders of magnitude lower than the $L_{\rm p} - E_{\rm p,z} - \Gamma_0$ relation of GRBs. The FSRQs and NLS1 seem to follow another tight relation which is different from that of GRBs.

We explore $L - E_{\rm syn,p} - \Gamma$ relation for each subclass of the AGNs, using the stepwise regression analysis method. Our model is $\log L^r(\log E_{\rm syn,p}, \log\Gamma) = a + b\log E_{\rm syn,p} + c\log\Gamma$. Our results are reported in Table 6 and shown in Figure 3. We do not find a $L - E_{\rm syn,p} - \Gamma$ relation with $p_{\rm F} < 10^{-4}$ for the BL Lacs, where $p_{\rm F}$ is the probability of the F-test for our regression analysis. Similar $L_{\rm syn} - E_{\rm syn,p} - \Gamma$ and $L_{\rm bol} - E_{\rm syn,p} - \Gamma$ relations are found for the FSRQs and NLS1 galaxies. Our regression analysis for the combined sample of the FSRQs and NLS1 galaxies yields $\log L_{\rm syn,52} = (-7.40 \pm 0.77) + (0.45 \pm 0.15)\log E_{\rm syn,z}/{\rm keV} + (3.50 \pm 0.25)\log\Gamma$ and $\log L_{\rm bol,52} = (-8.16 \pm 0.71) + (0.22 \pm 0.14)\log E_{\rm syn,z}/{\rm keV} + (4.48 \pm 0.23)\log\Gamma$, as shown in Figure 4. One can find that the dispersion of the three parameter relations is significantly tighter than the $L - \Gamma$ relations.

Table 4 Data of Our GRB Sample Taken from Liang et al. (2015)

GRB	z	T_{90} (s)	Γ_0	$\log(E_{\rm p,z})$ (keV)	$\log(L_{\rm p,52})$ (erg s^{-1})	$\log(L_{\rm bol,52})$ (erg s^{-1})
990123	1.6	63.3 ± 0.26	600 ± 80	3.13 ± 0.02	1.44 ± 0.02	0.75 ± 0.01
090924	0.544	48 ± 3	300 ± 79	2.44 ± 0.01	0.32 ± 0.03	-1.04 ± 0.03
080810	3.35	106 ± 5	409 ± 34	3.13 ± 0.10	0.98 ± 0.04	-0.42 ± 0.03
060605	3.78	15 ± 2	197 ± 30	2.69 ± 0.22	-0.02 ± 0.07	-0.72 ± 0.09
050820A	2.615	50 ± 5	282 ± 29	$2.95^{+0.22}_{-0.12}$	$0.51^{+0.04}_{-0.06}$	-0.50 ± 0.05
060607A	3.082	100 ± 5	296 ± 28	2.76 ± 0.15	0.30 ± 0.06	-1.05 ± 0.34
060418	1.489	52 ± 1	263 ± 23	$2.76^{+0.23}_{-0.06}$	0.28 ± 0.03	-0.56 ± 0.01
070208	1.165	48 ± 2	115 ± 23	$1.82^{+1.18}_{-0.22}$	-1.03 ± 0.05	-2.23 ± 0.34
081203A	2.1	294 ± 71	219 ± 21	3.19 ± 0.21	0.45 ± 0.03	-0.92 ± 0.11
070419A	0.97	116 ± 6	91 ± 11	$1.43^{+0.26}_{-0.31}$	-2.01 ± 0.04	-1.82 ± 0.43
060904B	0.703	192 ± 5	108 ± 10	2.13 ± 0.13	-1.13 ± 0.08	-2.72 ± 0.09
080710	0.845	120 ± 17	53 ± 8	$2.48^{+0.72}_{-0.29}$	-1.10 ± 0.04	-2.18 ± 0.44
080319C	1.95	34 ± 9	228 ± 5	3.24 ± 0.13	0.98 ± 0.01	-0.36 ± 0.12
071010B	0.947	35.7 ± 0.5	209 ± 4	2.01 ± 0.05	-0.26 ± 0.02	-1.14 ± 0.03
070110	2.352	85 ± 5	127 ± 4	2.57 ± 0.20	-0.35 ± 0.07	-1.19 ± 0.12
060210	3.91	46 ± 10	264 ± 4	$2.86^{+1.17}_{-0.10}$	$0.87^{+0.12}_{-0.08}$	0.08 ± 0.17
061007	1.261	75 ± 5	436 ± 3	2.96 ± 0.02	$1.16^{+0.06}_{-0.07}$	0.10 ± 0.04
061121	1.314	81 ± 5	175 ± 2	3.11 ± 0.05	1.15 ± 0.01	-0.49 ± 0.06
090812	2.452	66.7 ± 14.7	501 ± 46	$3.30^{+0.19}_{-0.12}$	$1.00^{+0.04}_{-0.06}$	-0.20 ± 0.11
060218	0.0331	100 ± 10	2.3 ± 0.3	0.71 ± 0.03	-5.37 ± 0.16	-5.03 ± 0.06
100621A	0.542	63.6 ± 1.7	52.0 ± 4.8	2.16 ± 0.07	-0.50 ± 0.03	-1.16 ± 0.05
050922C	2.198	5 ± 1	274 ± 25	$2.80^{+0.14}_{-0.08}$	$0.82^{+0.02}_{-0.03}$	0.04 ± 0.09
091029	2.752	39.2 ± 5.0	221 ± 20	2.36 ± 0.13	0.24 ± 0.03	0.62 ± 0.07
071112C	0.822	15 ± 2	244 ± 22	$2.63^{+0.14}_{-0.09}$	0.02 ± 0.04	-0.84 ± 0.13
080129	4.394	48 ± 10	65 ± 6	$3.13^{+0.85}_{-0.26}$	0.43 ± 0.04	-0.84 ± 0.13
081109A	0.98	190 ± 60	68 ± 7	$2.32^{+0.63}_{-0.10}$	-0.71 ± 0.06	-1.67 ± 0.25
081008	1.967	185.5 ± 40.3	250 ± 23	$2.43^{+0.55}_{-0.10}$	-0.26 ± 0.01	-1.44 ± 0.14
091024	1.092	109.8 ± 16.7	69 ± 6	2.90 ± 0.13	0.21 ± 0.10	-0.59 ± 0.08
090102	1.547	27.0 ± 2.2	61 ± 6	$3.06^{+0.07}_{-0.06}$	0.77 ± 0.06	-0.10 ± 0.05
110205A	2.22	257 ± 25	177 ± 16	2.85 ± 0.15	0.40 ± 0.06	-0.66 ± 0.06
121217A	3.1	778 ± 16	247 ± 23	2.88 ± 0.13	0.55 ± 0.07	-1.10 ± 0.10
100728B	2.106	12.1 ± 2.4	373 ± 34	2.61 ± 0.03	0.27 ± 0.03	-0.61 ± 0.10
110213A	1.46	48 ± 16	223 ± 21	2.38 ± 0.02	0.32 ± 0.01	-0.88 ± 0.15
100906A	1.727	114.4 ± 1.6	369 ± 34	2.20 ± 0.04	0.39 ± 0.02	-0.53 ± 0.04

T_{90} is the GRB duration, Γ_0 is the initial Lorentz factor of the GRB firballs, $E_{\rm p,z}$ is the peak photon energy of the GRBs derived from the fits with the Band function (Band et al. 1993) in the burst frame, $L_{\rm p}$ and $L_{\rm bol}$ are the luminosity at the 1-second peak time slice and the time-integrated luminosity in the burst duration, respectively.

Table 5 Results of Our Spearman Linear Correlation Analysis for the AGNs and GRBs in Our Samples

Relation	Source	Expression	r	p	Δ
$L_{\rm syn}(\Gamma)$	FSRQs	$L_{\rm syn,52} = 10^{(-9.04\pm0.68)}\,\Gamma^{(3.33\pm0.57)}$	0.79	$< 10^{-4}$	0.39
	BL Lacs	$L_{\rm syn,52} = 10^{(-9.51\pm0.63)}\,\Gamma^{(2.27\pm0.51)}$	0.69	2.14×10^{-4}	0.64
	NLS1	$L_{\rm syn,52} = 10^{(-9.71\pm0.37)}\,\Gamma^{(3.89\pm0.41)}$	0.93	$< 10^{-4}$	0.34
	AGN+GRB	$L_{\rm syn,52} = 10^{(-10.88\pm0.32)}\,\Gamma^{(4.64\pm0.20)}$	0.92	$< 10^{-4}$	1.20
$L_{\rm bol}(\Gamma)$	FSRQs	$L_{\rm bol,52} = 10^{(-9.13\pm0.45)}\,\Gamma^{(4.58\pm0.38)}$	0.93	$< 10^{-4}$	0.26
	BL Lacs	$L_{\rm bol,52} = 10^{(-8.57\pm0.70)}\,\Gamma^{(2.32\pm0.57)}$	0.66	4.87×10^{-4}	0.71
	NLS1	$L_{\rm bol,52} = 10^{(-8.87\pm0.40)}\,\Gamma^{(4.13\pm0.43)}$	0.93	$< 10^{-4}$	0.36
	AGN+GRB	$L_{\rm bol,52} = 10^{(-8.29\pm0.27)}\,\Gamma^{(3.20\pm0.17)}$	0.89	$< 10^{-4}$	1.03
$E_{\rm syn,z}(\Gamma)$	FSRQs	$E_{\rm syn,z} = 10^{(-4.01\pm0.49)}\,\Gamma^{(-0.03\pm0.41)}$	0.02	0.94	-
	BL Lacs	$E_{\rm syn,z} = 10^{(1.34\pm1.17)}\,\Gamma^{(-1.86\pm0.96)}$	–0.38	0.06	-
	NLS1	$E_{\rm syn,z} = 10^{(-4.16\pm0.33)}\,\Gamma^{(-0.34\pm0.36)}$	–0.24	0.34	-
$L_{\rm syn}(E_{\rm syn,z})$	FSRQs	$L_{\rm syn,52} = 10^{(-1.83\pm1.82)}\,E_{\rm syn,z}^{(0.82\pm0.46)}$	0.36	0.09	-
	BL Lacs	$L_{\rm syn,52} = 10^{(-6.84\pm0.22)}\,E_{\rm syn,z}^{(-0.05\pm0.14)}$	–0.08	0.71	-
	NLS1	$L_{\rm syn,52} = 10^{(-7.06\pm3.39)}\,E_{\rm syn,z}^{(-0.19\pm0.76)}$	–0.06	0.81	-
$L_{\rm bol}(E_{\rm syn,z})$	FSRQs	$L_{\rm bol,52} = 10^{-3.03\pm2.25}\,E_{\rm syn,z}^{0.17\pm0.57}$	0.07	0.76	-
	BL Lacs	$L_{\rm bol,52} = 10^{-5.92\pm0.23}\,E_{\rm syn,z}^{0.16\pm0.15}$	–0.22	0.30	-
	NLS1	$L_{\rm bol,52} = 10^{-7.97\pm3.54}\,E_{\rm syn,z}^{-0.63\pm0.79}$	–0.20	0.44	-

r and p are the linear correlation coefficient and chance probability, and Δ is the 1σ dispersion of the pair correlation.

Table 6 Results of our linear regression analysis with a model of $\log L = a + b \log E + c \log \Gamma$ in the source frame for the AGNs (or GRBs) in our samples.

Relation	Source	Expression	$p_{\rm F}^a$	r^b	p^b	Δ^b
$L^r_{\rm syn}(E_{\rm syn,z},\Gamma)$	FSRQs	$L^r_{\rm syn,52} = 10^{(-5.86\pm1.78)} E^{(0.79\pm0.26)}_{\rm syn,z} \Gamma^{(3.31\pm0.48)}$	1.36×10^{-6}	0.86	$<10^{-4}$	0.27
	BL Lacs	$L^r_{\rm syn,52} = 10^{(-9.71\pm0.64)} E^{(0.15\pm0.11)}_{\rm syn,z} \Gamma^{(2.54\pm0.55)}$	5.62×10^{-4}	0.71	$<10^{-4}$	0.44
	NLS1	$L^r_{\rm syn,52} = 10^{(-7.58\pm1.19)} E^{(0.51\pm0.27)}_{\rm syn,z} \Gamma^{(4.07\pm0.39)}$	2.39×10^{-7}	0.94	$<10^{-4}$	0.28
	FSRQs+NLS1	$L^r_{\rm syn,52} = 10^{(-7.40\pm0.77)} E^{(0.45\pm0.15)}_{\rm syn,z} \Gamma^{(3.50\pm0.25)}$	0	0.94	$<10^{-4}$	0.30
$L^r_{\rm bol}(E_{\rm syn,z},\Gamma)$	FSRQs	$L^r_{\rm bol,52} = 10^{-8.59\pm0.94} E^{0.13\pm0.20}_{\rm syn,z} \Gamma^{4.57\pm0.38}$	8.11×10^{-10}	0.94	$<10^{-4}$	0.23
	BL Lacs	$L^r_{\rm bol,52} = 10^{-8.60\pm0.73} E^{0.03\pm0.13}_{\rm syn,z} \Gamma^{2.37\pm0.63}$	2.6×10^{-3}	0.67	4.77×10^{-4}	0.47
	NLS1	$L^r_{\rm bol,52} = 10^{-8.51\pm1.40} E^{0.09\pm0.32}_{\rm syn,z} \Gamma^{4.17\pm0.46}$	1.03×10^{-6}	0.93	$<10^{-4}$	0.33
	FSRQs+NLS1	$L^r_{\rm bol,52} = 10^{(-8.16\pm0.71)} E^{(0.22\pm0.14)}_{\rm syn,z} \Gamma^{(4.48\pm0.23)}$	0	0.96	$<10^{-4}$	0.29

[a] $p_{\rm F}$ is the probability of the F-test for our linear regression analysis results. [b] r and p are the linear correlation coefficient and chance probability derived from the Spearman correlation analysis for each pair of $L_{\rm r}$ and L. Δ is the 1σ dispersion of the pair correlation.

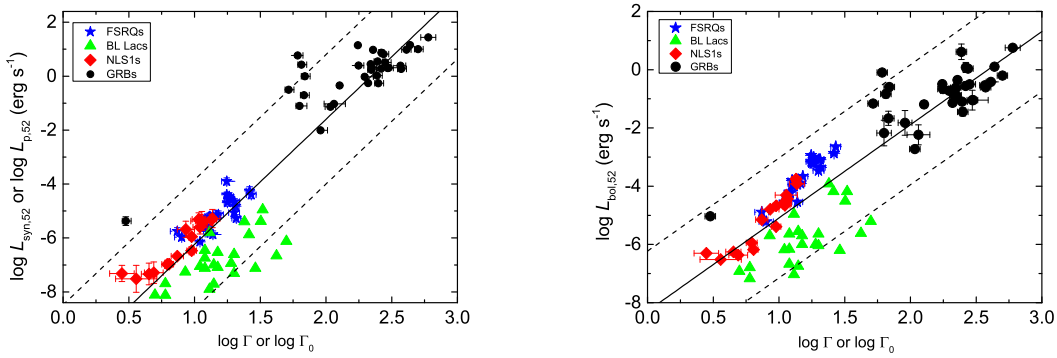

Fig. 1 Synchrotron peak luminosity and bolometric luminosity in the observed frames as a function of the jet Lorentz factor for the AGNs in our samples. GRBs in our sample are illustrated accordingly with their 1-second peak time luminosity ($L_{\rm p}$), time-integrated luminosity in the energy band of $1-10^4$ keV. *Lines* are the best fit and the 2σ dispersion derived from the Spearman linear correlation analysis for both the AGNs and GRBs.

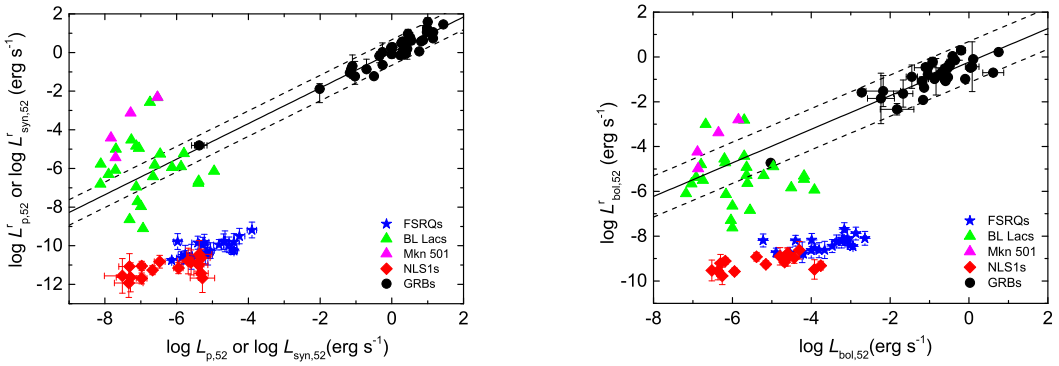

Fig. 2 Examination of whether or not the jet radiations of the AGNs share the same $L-E_{\rm p}-\Gamma_0$ relation as that derived from GRBs, in which $L^{\rm r}_{\rm syn}$ and $L^{\rm r}_{\rm bol}$ are calculated with the relations of $L^{\rm r}_{\rm p}(E_{\rm p},\Gamma_0)$ or $L^{\rm r}_{\rm bol}(E_{\rm p},\Gamma_0)$ derived from the GRB sample. The best linear fit line together with their 2σ dispersion regions of the relations are shown with *solid* and *dashed lines*, respectively (e.g., Liang et al. 2015). The pink triangles are the data for Mkn 501 in different outbursts taken from Zhang et al. (2013b).

4 CONCLUSIONS AND DISCUSSION

We have presented our analysis on the Doppler boosting effect on the observed luminosity and photon energy in AGNs and GRBs. Our analysis shows $L_{\rm syn} \propto \Gamma^{2.27\sim4}$ for the individual samples of the FSRQs, BL Lacs, and NLS1 galaxies. Similar relations are also found for $L_{\rm bol}(\Gamma)$. They also globally follow the same $L-\Gamma$ relation as $L \propto \Gamma^{4.64\pm0.20}$ together with the GRBs. A tight relation

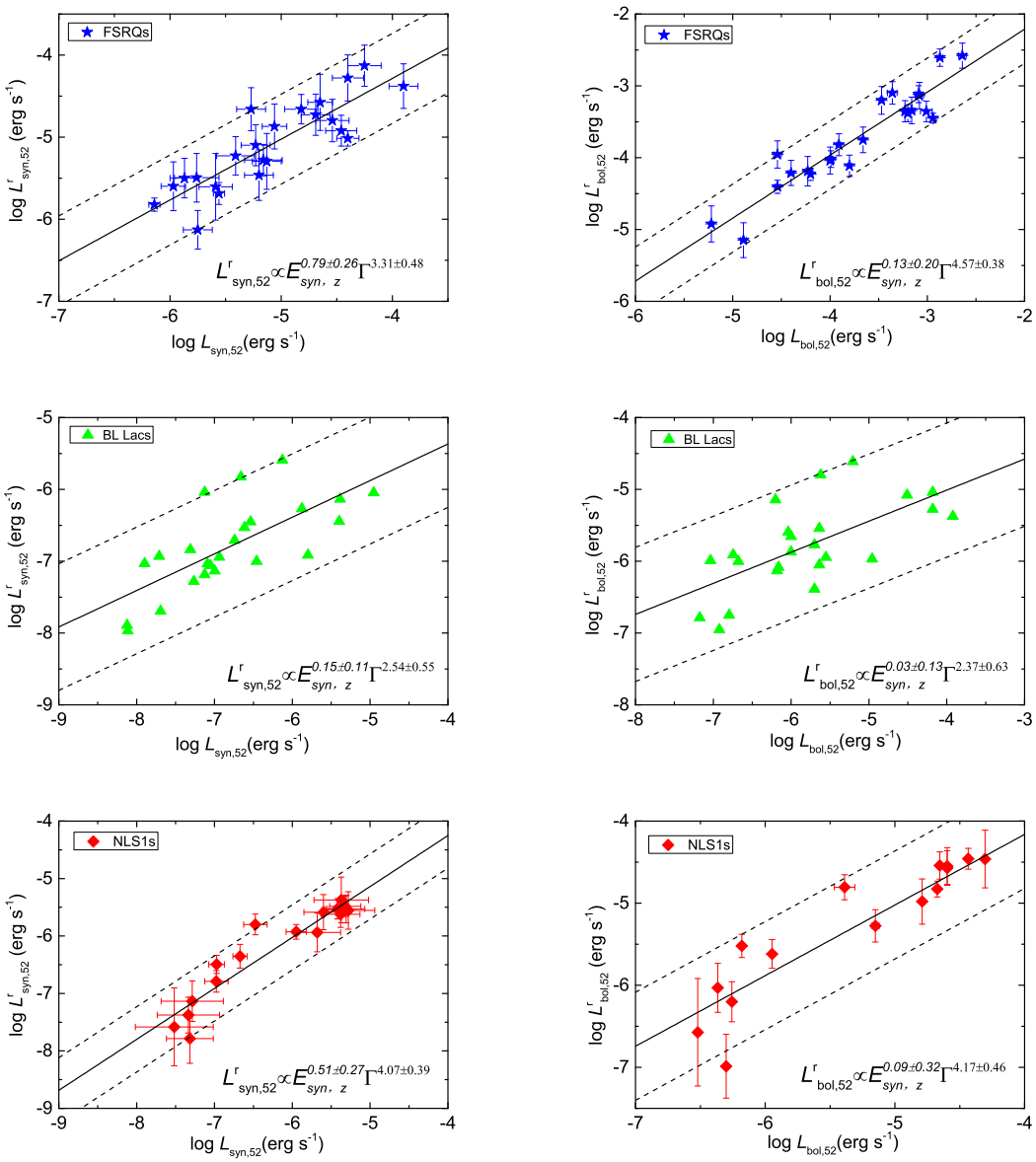

Fig. 3 Pair correlations of $\log L^{\rm r}_{\rm syn} - \log L_{\rm syn}$ and $\log L^{\rm r}_{\rm bol} - \log L_{\rm bol}$ planes, where $L^{\rm r}_{\rm syn}$ and $L^{\rm r}_{\rm bol}$ are calculated with the relations of $L^{\rm r}_{\rm syn}(E_{\rm syn,p},\Gamma)$ or $L^{\rm r}_{\rm bol}(E_{\rm syn,p},\Gamma)$ derived from each subclasses of AGN samples, as marked in each panels. The best linear fit line together with their 2σ dispersion regions of the relations are shown with *solid* and *dashed lines*, respectively.

$L_{\rm syn} \propto E^{0.45\pm0.15}_{\rm syn,z}\Gamma^{3.50\pm0.25}$ is found in the combined sample of FSRQs and NLS1 galaxies. This relation is different from that derived from the GRB sample.

As shown in Lyu et al. (2014), the different distributions of GRBs and blazars in the $L_{\rm syn}({\rm or}\ L_{\rm p}) - E_{\rm syn}({\rm or}\ E_{\rm p,z})$ plane may be due to both different radiation physics and jet environments. In addition, blazars have violent variability and a tentative flux-$E_{\rm syn}$ positive correlation is found in some blazars, such as 3C 279 and Mkn 501 (e.g., Zhang et al. 2013b; Wang et al. 2019). Taking the $L_{\rm syn}$, $E_{\rm syn}$, and δ values of Mkn 501 from Zhang et al. (2013b), we show Mkn 501 in four bright outbursts in Figure 2. One can find that it deviates the $L_{\rm p} - E_{\rm p,z} - \Gamma_0$ relation of GRBs in these outbursts. Wang et al. (2019) studied the $L_{\rm p}$-$E_{\rm p}$ relation of the Mkn 501 in different outbursts in a broad temporal coverage. They found that a weak $L_{\rm syn} - E_{\rm syn,z}$ correlation in some outbursts. We further examine whether it follows the $L_{\rm p} - E_{\rm p,z}$ relation within individual GRBs (Liang et al. 2004; Lu et al. 2012) in these outbursts. As shown in Figure 5, it still does not follow the $L_{\rm p} - E_{\rm p,z}$ relation of GRBs.

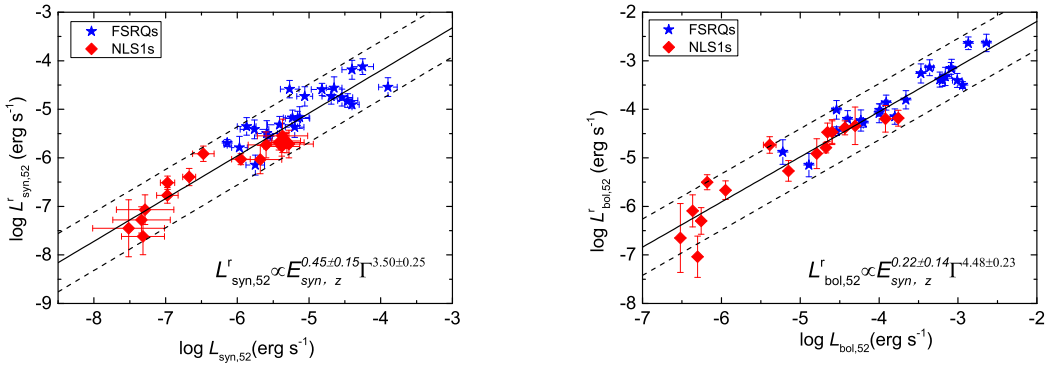

Fig. 4 The same as Fig. 2 but for the combined sample of the FSRQs and NLS1s.

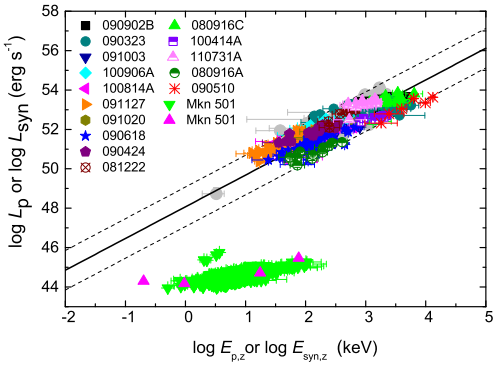

Fig. 5 $L_{\rm syn} - E_{\rm syn,z}$ relation of Mkn 501 in different outbursts in comparison to the $L_{\rm p} - E_{\rm p,z}$ relation within individual GRBs in different time slices. The data of Mkn 501 are taken from Zhang et al. (2013b) (the *pink triangles*) and Wang et al. (2019) (the *green triangles*). The GRB data are taken from Lu et al. (2012).

The observed luminosity is boosted by a factor of $\Gamma^{\rm p}$, where $p = 2+\beta$ for a continuous jet, $p = 3+\beta$ for a moving sphere, and β is spectral index of the synchrotron radiation emission (Ghisellini et al. 1993). Our analysis results for the different sub-classes of AGNs are consistent with the prediction of the Doppler boosting effect. The dependence of L on Γ in the $L-E_{\rm syn,p}-\Gamma$ relation of the FSRQs and NLS1 galaxies is still consistent with this prediction. However, the dependence of L on Γ for the GRBs significantly deviate this prediction. This may be due to the initial Lorentz factor Γ_0 is not a true representative of the bulk motion of the radiating region. The Γ_0 values in this analysis are the Lorentz factor of the forward shocked medium derived from the fireball deceleration time (the afterglow onset peak time) based on the standard afterglow model (e.g., Sari et al. 1998). In addition, GRB jets are episodic. They are composed of erratic shells with different initial Lorentz factor since their energy input and baryon matter loaded may be different. Therefore, the Γ_0 values derived form the afterglow data may not be the true Lorentz factor of the radiating region of the prompt gamma-rays. For example, Wang et al. (2000) inferred that the initial Lorentz factor of the fireball of GRB 990123 is 1200 and the Lorentz factor at its prompt optical emission peak time is 300.

Nemmen et al. (2012) illustrated that GRB jet luminosity is correlated with the jet power, and this relation is consistent with the correlation between jet power and the synchrotron peak luminosity of some AGNs (see also Zhang et al. 2013a; Wang et al. 2014). Note that a substantial fraction of the kinetic energy of the baryons should transferred to a non-thermal population of relativistic electrons through Fermi acceleration in the shock (e.g., Meszaros & Rees 1993). $L_{\rm p}$ is almost proportional to Γ_0 is within the error of the power-law index in the $L_{\rm p} - E_{\rm p,z} - \Gamma_0$ relation. We suspect that Γ_0 may be a representative of the kinetic power, or at least the power carried by the radiating electrons, in the radiating region (jet or jet patch). As discussed in Lyu et al. (2014), the different $L - E_{\rm p}$ relation in GRBs and blazars may be resulted from different scenarios of synchrotron radiations. The tight $L_p - E_{\rm p,z} - \Gamma_0$ relation may suggest that the observed

gamma-ray luminosity of GRBs depends on the radiation physics and the jet power together.

Acknowledgements We appreciate helpful comments from the anonymous referee. We thank J. Zhang, Y. J. Wang, and Y. Q. Xue for providing the data of Mkn 501 and suggestive discussion. This work is supported by the National Natural Science Foundation of China (Grant Nos. 11533003, 11851304 and U1731239), Guangxi Science Foundation and special funding for Guangxi distinguished professors (2017AD22006).

References

Abdo, A. A., Ackermann, M., Ajello, M., et al. 2009, ApJL, 707, L142
Amati, L., Frontera, F., Tavani, M., et al. 2002, A&A, 390, 81
Band, D., Matteson, J., Ford, L., et al. 1993, ApJ, 413, 281
Eichler, D., Livio, M., Piran, T., et al. 1989, Nature, 340, 126
Ghirlanda, G., Ghisellini, G., & Lazzati, D. 2004, ApJ, 616, 331
Ghisellini, G., Celotti, A., Fossati, G., et al. 1998, MNRAS, 301, 451
Ghisellini, G., Maraschi, L., & Dondi, L. 1996, A&AS, 120, 503
Ghisellini, G., Padovani, P., Celotti, A., & Maraschi, L. 1993, ApJ, 407, 65
Ghisellini, G., Tavecchio, F., & Ghirlanda, G. 2009, MNRAS, 399, 2041
Kobayashi, S., Piran, T., & Sari, R. 1999, ApJ, 513, 669
Kumar, P., & Zhang, B. 2015, Phys. Rep., 561, 1
Lü, J., Zou, Y.-C., Lei, W.-H., et al. 2012, ApJ, 751, 49
Liang, E. W., Dai, Z. G., & Wu, X. F. 2004, ApJL, 606, L29
Liang, E.-W., Lin, T.-T., Lü, J., et al. 2015, ApJ, 813, 116
Liang, E.-W., Yi, S.-X., Zhang, J., et al. 2010, ApJ, 725, 2209
Lithwick, Y., & Sari, R. 2001, ApJ, 555, 540
Lu, R.-J., Wei, J.-J., Liang, E.-W., et al. 2012, ApJ, 756, 112
Lyu, F., Liang, E.-W., Liang, Y.-F., et al. 2014, ApJ, 793, 36
Ma, R., Xie, F.-G., & Hou, S. 2014, ApJL, 780, L14
Maraschi, L., Ghisellini, G., & Celotti, A. 1992, ApJL, 397, L5
Massaro, F., Tramacere, A., Cavaliere, A., et al. 2008, A&A, 478, 395
Meszaros, P., & Rees, M. J. 1993, ApJ, 405, 278
Nemmen, R. S., Georganopoulos, M., Guiriec, S., et al. 2012, Science, 338, 1445
Pe'er, A., Ryde, F., Wijers, R. A. M. J., Mészáros, P., & Rees, M. J. 2007, ApJL, 664, L1
Peng, F.-K., Liang, E.-W., Wang, X.-Y., et al. 2014, ApJ, 795, 155
Paczynski, B. 1991, Acta Astronomica, 41, 257
Richards, J. L., & Lister, M. L. 2015, ApJL, 800, L8
Sari, R., & Piran, T. 1999, ApJ, 520, 641
Sari, R., Piran, T., & Halpern, J. P. 1999, ApJL, 519, L17
Sari, R., Piran, T., & Narayan, R. 1998, ApJL, 497, L17
Sikora, M., Begelman, M. C., & Rees, M. J. 1994, ApJ, 421, 153
Sikora, M., Stawarz, Ł., Moderski, R., Nalewajko, K., & Madejski, G. M. 2009, ApJ, 704, 38
Sun, X.-N., Zhang, J., Lin, D.-B., et al. 2015, ApJ, 798, 43
Tang, Q.-W., Peng, F.-K., Wang, X.-Y., & Tam, P.-H. T. 2015, ApJ, 806, 194
Tramacere, A., Giommi, P., Perri, M., et al. 2009, A&A, 501, 879
Urry, C. M., Falomo, R., Scarpa, R., et al. 1999, ApJ, 512, 88
Urry, C. M., & Padovani, P. 1995, PASP, 107, 803
Wang, F. Y., Yi, S. X., & Dai, Z. G. 2014, ApJL, 786, L8
Wang, J., & Wei, J. Y. 2011, ApJL, 726, L4
Wang, X. Y., Dai, Z. G., & Lu, T. 2000, MNRAS, 319, 1159
Wang, Y., Zhu, S., Xue, Y., et al. 2019, ApJ, 885, 8
Woosley, S. E. 1993, ApJ, 405, 273
Wu, Q., Zou, Y.-C., Cao, X., Wang, D.-X., & Chen, L. 2011, ApJL, 740, L21
Yonetoku, D., Murakami, T., Nakamura, T., et al. 2004, ApJ, 609, 935
Zhang, J., Liang, E.-W., Sun, X.-N., et al. 2013a, ApJL, 774, L5
Zhang, J., Liang, E.-W., Zhang, S.-N., & Bai, J. M. 2012, ApJ, 752, 157
Zhang, J., Sun, X.-N., Liang, E.-W., et al. 2014, ApJ, 788, 104
Zhang, J., Xue, Z.-W., He, J.-J., Liang, E.-W., & Zhang, S.-N. 2015, ApJ, 807, 51
Zhang, J., Zhang, S.-N., & Liang, E.-W. 2013b, ApJ, 767, 8
Zhang, X., Zhang, H., Zhang, X., et al. 2017, Ap&SS, 362, 224
Zou, Y.-C., Cheng, K. S., & Wang, F. Y. 2015, ApJL, 800, L23
Zhu, B.-T., Zhang, L., & Fang, J. 2019, ApJ, 873, 120
Zhu, Y.-K., Zhang, J., Zhang, H.-M., et al. 2016, RAA (Research in Astronomy and Astrophysics), 16, 170